*SF2A 2014*
*J. Ballet, F. Bournaud, F. Martins, R. Monier and C. Reylé (eds)*

# THE ROLE OF NEUTRON STAR MERGERS AND CORE COLLAPSE SUPERNOVAE IN R PROCESS NUCLEOSYNTHESIS

F. Daigne[1] and E. Vangioni[1]

**Abstract.** Recent IR/optical/UV observations and Gamma-ray burst rate determinations at high redshift have led to significant progress in establishing the cosmic evolution of the star formation rate density (SFRD). The SFRD is then used to predict the ionization history of the Universe, and the evolution of the cosmic chemical abundances, supernova rates, etc, as a function of the redshift z. These predictions are done in the framework of the hierarchical model for structure formation. In this context, we focus here our attention on the origin and evolution of a typical r process element: Europium, in two possible sites: core collapse supernovae (SNII) or Neutron Star Mergers (NSM). In the first scenario, there is only one parameter, the yield of Eu produced in these SNII. In the second one, there are three physical parameters, Eu yield, binary star fraction and time delay before the merger. The comparison of our results with available observations of Eu in stars at various metallicities strongly favors the NSM site for the r process. In addition, it allows to put a constraint on the time delay for mergers, which is typically 0.1-0.2 Gyr, and to make an independent prediction for the expected rate of mergers in the horizon of the adv Virgo/Ligo detectors, which we find typically to be of the order of 3 to 10 events per year for NS/NS and NS/BH mergers respectively.

Keywords: R process nucleosynthesis, neutron star mergers, supernovae, cosmic chemical evolution.

## 1 Introduction

The r-process, or rapid neutron-capture process, of stellar nucleosynthesis is invoked to explain the production of the stable neutron-rich nuclides heavier than iron. They are observed in stars of different metallicities, including in very low metalllicity stars (Roederer *et al.* 2014). However, despite a growing wealth of observational data (Francois *et al.* 2007; Ren *et al.* 2012; Roederer *et al.* 2012), and although increasingly better r-process models are developed with new astrophysical or nuclear physics ingredients, the astrophysical site of r-process is not clearly identified. Presently, two scenarios are considered. The first scenario (SNII site) is directly correlated to the global star formation rate (SFR). The second scenario, neutron star - neutron star and neutron star - black hole mergers (NSM) is from now on the favored site due to the new comprehensive nucleosynthesis analysis for ejecta of compact binaries (Goriely *et al.* 2011; Bauswein *et al.* 2013; Just *et al.* 2014).

## 2 Cosmic chemical evolution

We follow the cosmic chemical evolution using a semi-analytical model which reproduces the cosmic star formation rate in the cosmological context of hierarchical structure formation (standard Press-Schechter (PS) formalism, Press & Schechter 1974). Our model tracks baryons (i) in stars or their remnants within collapsed structures; (ii) in the gas within collapsed structures (the interstellar medium, ISM); (iii) in the gas outside of structures (the intergalactic medium, IGM). The model includes mass (baryon) exchange between the IGM and ISM (structure formation, galactic outflows), and between the ISM and the stellar component (star formation, stellar explosions). We assume the following cosmological parameters $\Omega_m = 0.27, \Omega_\Lambda = 0.73$ and $H_0 = 71$ km/s/Mpc (h = 0.71). This model allows to compute the evolution of many important quantities as a function of redshift, including stellar explosion rates and the cosmic abundances of several chemical elements. For details see Daigne *et al.* (2006); Rollinde *et al.* (2009).

[1] UPMC-CNRS, UMR7095, Institut d'Astrophysique de Paris, 75014 Paris, France

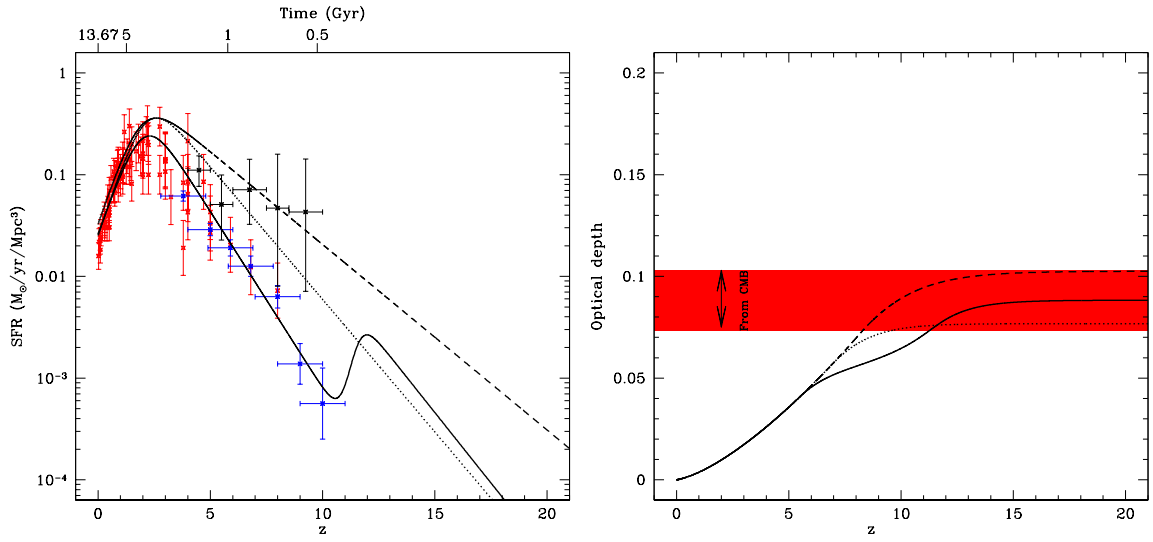


**Fig. 1. Left:** Cosmic SFR as a function of redshift for the three cases considered in our study (see text): SFR1, a standard SFR with a massive mode at high redshift (solid line); SFR2, a flattened standard SFR (dotted line); and SFR3, an extreme flattened standard SFR (dashed line). The observational constraints are also plotted (Behroozi *et al.* 2013, red points; Oesch *et al.* 2013a; Bouwens *et al.* 2014 and references therein, blue points; Kistler *et al.* 2013, black points). **Right:** For each of the three cases of SFR plotted on the left side (same line styles), the evolution of the Thomson optical depth due to free electrons in the IGM is plotted as a function of redshift. The constraint on this optical depth from CMB measurements is indicated by a red strip (WMAP9 results, Hinshaw *et al.* 2013).

In the following, we consider three distinct modes of star formation: (i) SFR1, a standard mode of Population II/I stars correlated to star forming galaxy observations (Behroozi *et al.* 2013; Oesch *et al.* 2013a; Bouwens *et al.* 2014), together with a more massive mode (Population III stars) at high redshift; (ii) SFR2, a flattened standard SFR; and (iii) SFR3, an extreme flattened standard SFR, correlated to recent measurements derived from the cosmic gamma ray burst rate (Kistler *et al.* 2013). In addition to these prescriptions for the formation rate, we adopt an IMF with a single Salpeter slope ($x = 1.35$), and a mass range 0.1-100 $M_\odot$ for the standard Pop II/I stars (SFR1-3) and 36-100 $M_\odot$ for the massive Pop III stars (SFR1). More details on these assumptions can be found in Vangioni *et al.* (2014a,b). These three cases are plotted on the left panel in Figure 1, together with the observational constraints cited above.

Predictions obtained with these three SFRD modes are compared with several observational constraints. We find a good agreement with the CMB constraint on the reionization of the IGM (see right panel in Figure 1); with the evolution of the rate of core-collapse and thermonuclear supernovae; with the evolution of the cosmic abundances of several chemical elements (C,O, Mg, Si, Fe) both in the ISM and the IGM. More details on the model and the comparison to observations can be found in (Daigne *et al.* 2006; Rollinde *et al.* 2009; Vangioni *et al.* 2014a,b). In this paper, we focus on the cosmic evolution of Europium, as a typical r process element.

## 3 Europium evolution: core collapse supernovae (SNII) vs mergers (NSM)

We compute the production of Eu, by assuming that it is produced either by core collapse supernovae (we assume a unique yield of $10^{-7}$ $M_\odot$ of Eu per explosion, for all progenitor masses and metallicities), or by NS/NS or NS/BH mergers. In the latter case, the model has three physical parameters: the Eu Yield (7 to 20 $10^{-5}$ $M_\odot$, Just *et al.* 2014), the time delay between the formation of the neutron stars and the merger, and the fraction of neutron stars which are in a NS/NS or a NS/BH binary system leading to a merger (0.002).

We find that observations of Europium at [Fe/H] > -2.5 are well reproduced by both scenarios. On the other hand, the situation is very different at low metallicity, where the observed evolution of Europium clearly favors mergers as the main astrophysical site for the r process. Indeed, as shown in Figure 3, Eu is overproduced at high z/low metallicity in the core collapse supernova scenario, whereas the observed decrease of Eu/H for [Fe/H] < -2.5 is reproduced by mergers, due to the time delay between star formation and mergers, which is then constrained to be in the 0.1-0.2 Gyr range. This result depends on the iron yield from supernovae, and on the existence or not of the Pop III star mode at high redshift. If more iron is produced at early time (high redshift), the time delay is constrained to be shorter (see Figure 2). Note that the supernova scenario can be reconciled

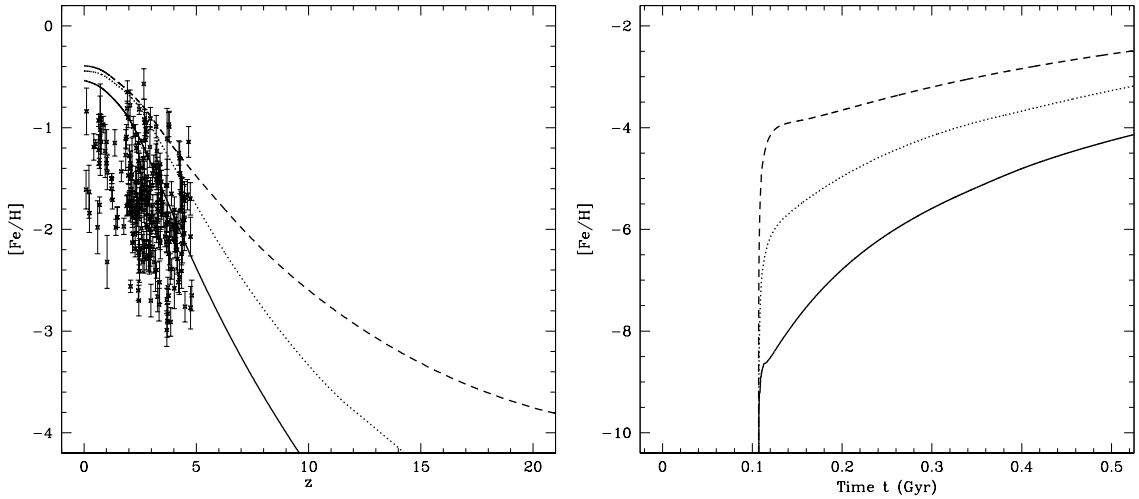


**Fig. 2. Left:** Iron evolution as a function of redshift z for the three SFR modes. Line styles are the same as in Figure 1. Measurements of the iron abundance in DLAs are also plotted (Rafelski *et al.* 2012). **Right:** Iron evolution as a function of time in the early Universe. Note that [Fe/H] can vary from -9 to -4, depending on the assumption for the SFRD.

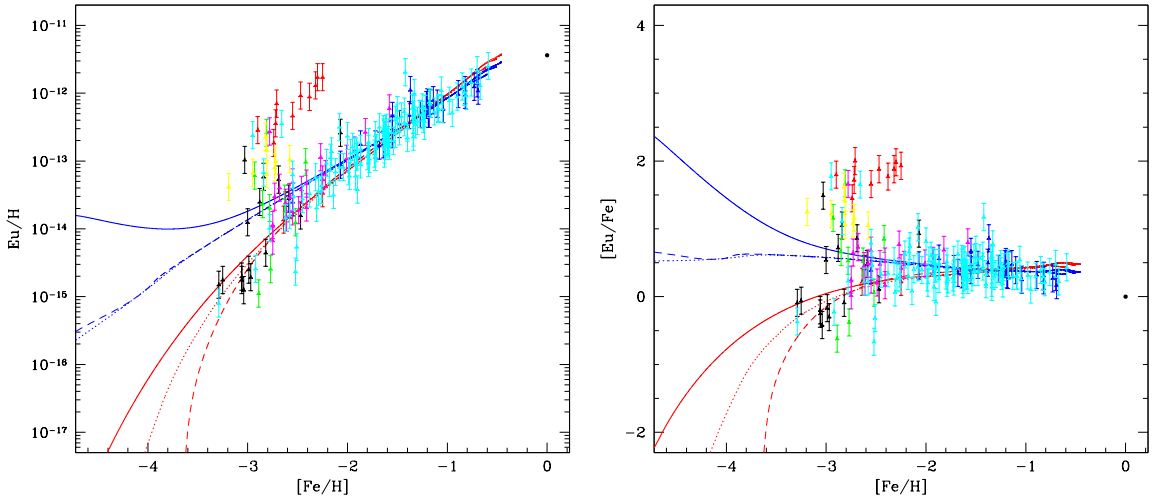


**Fig. 3. Left:** Evolution of Eu/H as a function of [Fe/H]. Blue lines represent the evolution of Eu in the SNII progenitor case, red lines represent the NSM progenitor case, for the three SFR modes (same line styles as in Figure 1). In the merger scenario, the time delay is adjusted to fit the observations, leading to 0.2, 0.15, 0.1 Gyr for the SFR1, SFR2, SFR3 modes, respectively. The other parameters are given in the text. **Right:** [Eu/Fe] vs [Fe/H] for the three considered SFR modes and for SNII (blue lines) and NSM (red lines) sites.

with observations if it is assumed that Eu is produced only when the progenitor star has a metallicity $Z > 10^{-4}$ $Z_{\odot}$. Unfortunately, Eu observations at very low metallicities are missing to further test our conclusions. In the future, we will consider also another element, Ba, for which observations at [Fe/H] < -3 are available.

## 4 Conclusion

This work shows that the recent measurements of the Eu abundance in low metallicity stars leads to a cosmic evolution of this element which strongly favors NS/NS and NS/BH mergers as the main astrophysical site for the production of heavy elements by the r process. An interesting by-product of this study is the possibility to obtain an independent constraint on the merger rate in the Universe, thanks to the chemical evolution of r process elements. This is a key ingredient to predict detection rates by gravitational wave detectors. Our

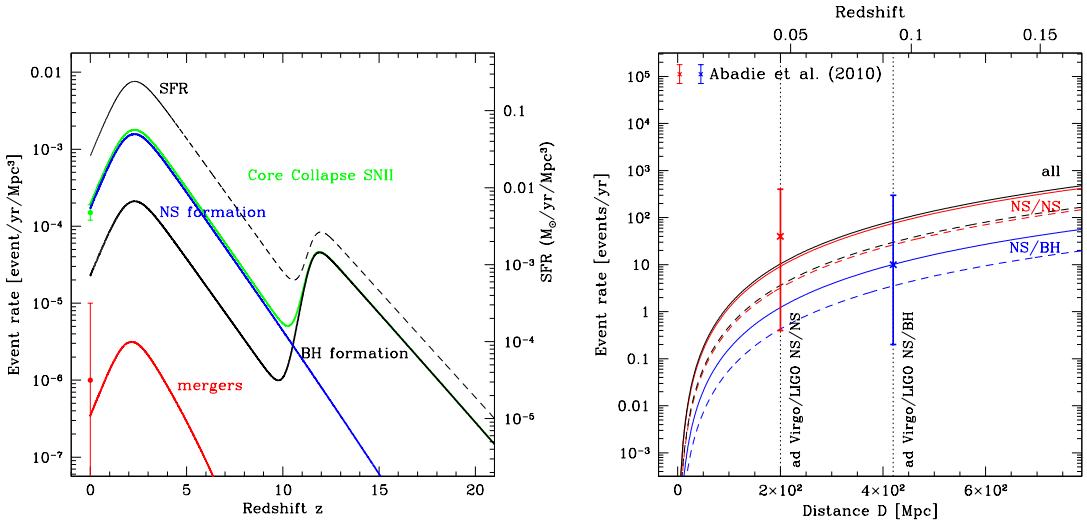


**Fig. 4. Left:** Star formation rate, birth rate of neutron stars (NS) and black holes (BH), core-collapse supernova rate (SNII), and NS/NS+NS/BH merger rate as a function of redshift, for the SFR1 mode. Green and red points represent the local SNII (Mattila *et al.* 2012) and merger (Abadie *et al.* 2010) rates, respectively. **Right:** integrated merger event rate (NS/NS, NS/BH and total) as a function of distance and redshift for the SFR1 mode. A comparison with Adv Virgo and Adv Ligo predictions is done (Abadie *et al.* 2010). Solid (resp. dashed) lines show the evolution with an Eu yield of 7 $10^{-5}$ $M_{\odot}$ (resp. 2 $10^{-4}$ $M_{\odot}$ ) and a fraction of mergers of 0.002 (resp. 0.0007). The time delay before coalescence is 0.2 Gyr in both cases.

result is plotted as a function of redshift in Figure 4, with a comparison to the predicted rates in the horizon of advanced Virgo/Ligo. The agreement is good with the mean values published by Abadie *et al.* (2010).

F.D. and E.V. acknowledge the Programme National Hautes Energies (PNHE) for financial support.

## References

Abadie, J. *et al.* 2010, Cl.Qu.Gr., 27, 173001
Bauswein, A., Goriely, S. & Janka, H.T 2013, ApJ773, 78
Behroozi, P. S., Wechsler, R. H., & Conroy, C. 2013, ApJ, 770, 57
Bouwens, R. J. *et al.* 2014, arXiv 1403.4295
Daigne, F., Olive, K. A., Silk, J., Stoehr, F., & Vangioni, E. 2006, ApJ, 647, 773
Francois, P. *et al.* 2007, A&A, 476, 935
Goriely, S., Bauswein, A. & Janka, H.S. 2011, ApJL, 738, L32
Hinshaw, G., Larson, D., Komatsu, E. *et al.* 2013, ApJS, 208, 19
Just, O. *et al.* 2014, arXiv1406.2687
Kistler, M.D. *et al.* 2013, arXiv1305.1630
Mattila, S., Dahlen, T., Efstathiou, A. *et al.* 2012, ApJ, 756, 111
Oesch, P. A., Bouwens, R. J., Illingworth, G. D. *et al.* 2013a, ApJ, 773, 75
Oesch, P. A., Bouwens, R. J., Illingworth, G. D. *et al.* 2013b, arXiv:1309.2280
Press, W. H., & Schechter, P. 1974, ApJ, 187, 425
Rafelski, M. *et al.* 2012, ApJ, 755, 89
Ren, M. *et al.* 2012, ApJ, 755, 89
Roederer, I.U. *et al.* 2012, ApJS, 203, 27
Roederer, I.U. *et al.* 2014, accepted in ApJ, arXiv1402.4144
Rollinde, E., Vangioni, E., Maurin, D., Olive, K. A., Daigne, F., Silk, J., & Vincent, F. H. 2009, MNRAS, 398, 1782
Vangioni, E. *et al.* 2014a arXiv1409.2462
Vangioni, E. *et al.* 2014b submitted